Accepted Manuscript

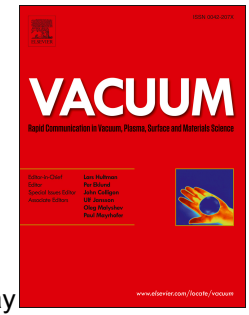

Facile synthesis and characterization of hydroxyapatite particles for high value nanocomposites and biomaterials

Florin Miculescu, Aura-Cătălina Mocanu, Cătălina Andreea Dascălu, Andreea Maidaniuc, Dan Batalu, Andrei Berbecaru, Stefan Ioan Voicu, Marian Miculescu, Vijay Kumar Thakur, Lucian Toma Ciocan

PII: S0042-207X(17)30594-8

DOI: 10.1016/j.vacuum.2017.06.008

Reference: VAC 7449

To appear in: *Vacuum*

Received Date: 12 May 2017

Revised Date: 30 May 2017

Accepted Date: 5 June 2017

Please cite this article as: Miculescu F, Mocanu Aura-Că ă, Dascălu CăăAndreea, Maidaniuc A, Batalu D, Berbecaru A, Voicu SI, Miculescu M, Thakur VK, Ciocan LT, Facile synthesis and characterization of hydroxyapatite particles for high value nanocomposites and biomaterials, *Vaccum* (2017), doi: 10.1016/ j.vacuum.2017.06.008.

Vacuum, Volume 146, December 2017, Pages 614-622
DOI:10.1016/j.vacuum.2017.06.008

Facile Synthesis and Characterization of Hydroxyapatite Particles for High Value Nanocomposites and Biomaterials

Florin Miculescu[a], Aura-Cătălina Mocanu[a,b], Cătălina Andreea Dascălu[a], Andreea Maidaniuc[a,c], Dan Batalu[a], Andrei Berbecaru[a], Stefan Ioan Voicu[d,] *, Marian Miculescu[a,] **, Vijay Kumar Thakur[e,] ***, Lucian Toma Ciocan[f]

[a] Faculty of Material Science and Engineering, University Politehnica of Bucharest, Splaiul Independentei 313, 011061 Bucharest, Romania.

[b] Research and Development Department, S.C.Nuclear NDT Research&Services S.R.L, Berceni Road 104, District 4, Bucharest, Romania

[c] Destructive and Nondestructive Testing Laboratory, S.C.Nuclear NDT Research&Services S.R.L, Berceni Road 104, District 4, Bucharest, Romania

[d] Faculty of Applied Chemistry and Material Science, University Politehnica of Bucharest, Gheorghe Polizu 1-7, 011061 Bucharest, Romania.

[e] School of Aerospace, Transport and Manufacturing, Cranfield University, College Road, Cranfield MK43 0AL, UK

[f] Faculty of Dental Medicine, University of Medicine and Pharmacy U.M.F. „Carol Davila", Calea Plevnei 17-23, 030167 Bucharest, Romania.

*Corresponding author: Stefan Ioan Voicu - svoicu@gmail.com, stefan.voicu@upb.ro

**Corresponding author: Marian Miculescu – m_miculescu@yahoo.com

***Corresponding author: Vijay Kumar Thakur - Vijay.Kumar@cranfield.ac.uk

Abstract:

Lately Hydroxyapatite has gained a lot of research interest and intense focus due to its structural as well as compositional similarity to the components of human bone mineral. The conversion of calcium-rich precursors to hydroxyapatite could lead to the development of a new sustainable alternative with a valuable environmental and socio-economically impact. Still, current approaches faces lots of challenges in terms of synthesis parameters compatible to a reproducible route for calcium phosphates (hydroxyapatite included) synthesis. The optimization of Rathje synthesis route and

characterization of biogenic derived calcium phosphates from dolomitic marble and *Mytilus galloprovincialis* seashells, constitutes the main goals of this study. The synthesized materials were characterized using FTIR, SEM coupled with EDS, and X-ray diffraction at all synthesis stages. Precursors were also subjected to thermal analysis and differential scanning calorimetry for thermal transformations investigations and dissociation temperature setting. This study suggests that acid quantity and magnetic stirring are the key-factors for Ca/P molar ratio adjustment, hence for the amount of naturally-derived hydroxyapatite. This research also contributes to the development of new strategies for further optimization of the conversion procedure and removal of residual components.

Keywords: Dolomitic marble and *Mytilus galloprovincialis* seashell; hydroxyapatite chemical precipitation; Ca/P molar ratio; hydroxyapatite phase-proportion; bi-phasic calcium phosphate

1. INTRODUCTION

Very recently different kinds of functional and sustainable materials are being explored for their usage in a number of applications ranging from biomedical, automotive to aerospace[1] [2,3] [4–6]. Especially in the field of biomedical, the ongoing tendencies in the clinico-surgical field are directed towards the development and promotion of a rising generation of ceramic biomaterials solely dedicated for bone restoration. These materials could constitute a hasty and complete solution for size-varied bone defects, especially for the extensive ones. Current reparatory techniques include allografts, autografts, metallic, ceramic and synthetic polymer materials, each one of them facing specific drawbacks [7] [8] [9–12]. In terms of calcium phosphates (CaPs) (Ca/P = 0.5-2.0), the most suitable one is stoichiometric hydroxyapatite (HA) (Ca/P =1.67), similar to natural apatite through its excellent biocompatibility, compressive strength and bioactivity. A more socio-economically engaging alternative targets the synthesis of new biomimetic substituents derived from widespread biogenic resources (e.g. mussel shell wastes from food industry) that are highly capable of bone-cavity breeding [13]. The possibility of an environmentally-friendly exploitation of marine resources to biological CaPs has emerged with the development of a coralline derived-HA synthesis method in 1974[14] [15]. For the high demand of bone substitute materials, current

replacements are being made by investigating another natural wastes: marine skeletons, different types of seashells, eggshells or sea urchins as precursors for biogenic HA synthesis[16] [17] [13]. Each of the mentioned materials is a polymorphic form of calcium carbonate ($CaCO_3$). Chemical conversion of $CaCO_3$ in CaPs can be carried out by: hydrothermal, mecano-chemical, sol-gel or precipitation techniques, based on two possibilities: *(i)* direct treatment of $CaCO_3$ with phosphor-based reagents (e.g. phosphoric acid, H_3PO_4), but the reaction involves temperatures of 150-200°C and setting times up to 6h or *(ii)* indirect route by thermal dissociation of $CaCO_3$ into calcium oxide (CaO) and its further treatment with phosphoric acid. Most of the reported indirect routes based on natural resources are hardly reproducible because of the incomplete synthesis parameters. Optimum dissociation temperature of $CaCO_3$ has not been exactly determined and in literature has been reported to be in the range of 600-1200°C[18][19]. The maximum/optimum reagent quantities used for the HA synthesis have also not been fully disclosed. Moreover, given the widespread of $CaCO_3$ sources, their environment can also influence the initial chemical composition and therefore the synthesized CaPs` phase proportion. Although the indirect route was developed by Rathje in 1939 for pure reagents [20], this study proposes a convenient adaptation for dolomitic marble and *Mytilus galloprovincialis* seashells conversion to CaPs. Marble processing stands as a new alternative for the extension of natural $CaCO_3$ – based materials range used for CaPs synthesis.

In order to achieve reproducible results, in this work, we have reported an exhaustive analysis and characterization for each step of the synthesis: *(i)* raw materials (marble and seashell), *(ii)* CaO intermediate powders and *(iii)* end products resulted after H_3PO_4 reaction. This characterization has been aimed for the HA`s stoichiometry control, particles` shape and dimension variation, powders` specific agglomeration prevention and removal of potentially cytotoxic compounds. Since morphological and structural characteristics of intermediate and final products (i.e. HA phase proportion) are dependent on the synthesis parameters, this research determines the influence of three major factors: *(a)* cooling parameters, *(b)* H_3PO_4 quantity and *(c)* magnetic stirring.

2. MATERIALS AND METHODS

2.1 *Samples preparation*

Ceramic materials were procured from two types of natural precursors: white autochthonous dolomitic marble (Ruşchița, România) and *Mytilus galloprovincialis* mussel shells (Marea Neagră, România). Marble slabs were cut into dimensions of 15 × 20 cm and the seashells were washed and scrubbed for sand particles removal. CaO powder was obtained as a result of precursors` calcination (**Eq. 1**) in an electric oven at 1300°C, for 6 h, followed by air cooling (**Fig. 1**). Subsequently, the samples were stored in sterile Petri dishes and exposed to atmospheric air for 6 months. CaO transformation to HA was conducted according to Rathje method (**Eq. 2&3**), optimized as shown in **Fig. 2**: *(a)* H_3PO_4 quantity was initially calculated based on chemical stoichiometry and gradually increased to 50%, *(b)* magnetic stirring was conducted at 25°C for 2h and *(c)* H_3PO_4 was drop-wise added at a rate of 1 ml/min. According to stoichiometric calculations, for 2g of CaO, 200 ml of distilled water and 1.33 ml of H_3PO_4 (95% solution, Sigma-Aldrich) was added. Samples were labeled based on H_3PO_4 quantity (e.g. 1 = stoichiometric quantity – 100%, 1.5 = 150% × calculated H_3PO_4 quantity) and the precursor used (M – marble, S – seashell). Sample 0-M was stoichiometrically prepared but in the absence of magnetic stirring (**Table 1**). Subsequently, the obtained solutions were filtered and dried in a two-step process: *(i)* for 24h at room temperature (RT) and *(ii)* in electric oven with air atmosphere, at 120°C, for 2 ½ h and then slowly cooled in the oven for 2h down to 40°C (**Fig. 2 & 3**). Samples were stored in Petri dishes and immediately sealed in the desiccator with silica gel.

2.2 Physico-chemical techniques for phased precursor and product characterization

Morpho-compositional characteristics were determined using scanning electron microscopy (SEM) (Philips Xl 30 ESEM TMP) that is coupled with energy-dispersive spectroscopy (EDS) (EDAX Sapphire spectrometer). EDS analysis was performed in five different areas. Thermal transformations of raw materials were investigated by simultaneous differential scanning calorimetry (DSC)/ thermal gravimetric analysis (TGA) on a TA instrument (SDT Q600) in a temperature range of 25 – 1500°C at a 10°C/min heating rate. The device chamber was purged with 20ml/min Ar flow rate. The pH values were recorded, after the completion of synthesis, with a pH-meter (Hanna Instruments – HI 254).

Crystallographic structure was evaluated by X-ray diffraction (XRD) with a Panalytical diffractometer, equipped with Cu K_α (λ = 1.5418 Å) radiation, at an accelerating voltage of 30kV and intensity of 25 mA. The scattered intensity was scanned in the 2θ range of 15-70°, with a step size of 0.02° and dwell time of 4s. The presence and the arrangement of functional groups were analyzed by Fourier Transform Infrared (FT-IR) spectroscopy, with a Bruker Tensor 27 (ATR diamond annex) spectrometer. The spectra were recorded in the 400-4000 cm^{-1} range, at a resolution of 4 cm^{-1} and an average of 32 consecutive scans/ sample.

3. RESULTS AND DISCUSSION

The dissociation reaction of calcium carbonate has been reported as follows (Eq. 1) [21] [22] :

$$CaCO_3 \xrightarrow{\pi} CaO + CO_2 \qquad \textbf{(Eq.1)}$$

The setting reaction between Ca $(OH)_2$ and H_3PO_4 develops exothermically with the controlled release of phosphate anions in the water, in three stages (reactants dissolution, new phase nucleation and the crystallization of the reaction products). Mixing these two solutions can lead to the precipitation of different calcium phosphates phases, depending on the reagent quantity and the pH of the resulting solution (Eq. 2&3)[18] . A gradual gelation of the aqueous solution has been observed until the mixing is performed with difficulty. This point corresponds to the gel crystallization stage around unreacted CaO particles[19] [20] .

$$CaO + H_2O \rightarrow Ca(OH)_2 \qquad \textbf{(Eq.2)}$$

$$10Ca(OH)_2 + 6H_3PO_4 \rightarrow Ca_{10}(PO_4)_6(OH)_2 + 18H_2O \qquad \textbf{(Eq.3)}$$

Gradual increment in the H_3PO_4 quantity results in the precipitation of more acidic compounds apart from HA. The most known one is brushite (DCPD) formed as a primary or secondary product after precipitation from calcium and phosphor-based solutions with moderate or neutral acidity. DCPD is considered a HA precursor and can remain stable, re-precipitate or dissolve during synthesis. The anhydrous form of brushite – monetite (DCPA) – can precipitate in higher acidic conditions (low pH values) from the synthesis outset [23]or is formed as a result of further processing stages

[24]. In the human body, only DCPD has been found in the non-collagen organic matter and is considered the "reservoir" of phosphate/ calcium ions that are prerequisite for subsequent mineralization[25].

3.1 Biogenic resources characterization

Fig. 3 shows the comparative morpho-structural characteristics of raw precursors. The morphological analysis highlighted *(i)* a layered and compact structure in both cases and *(ii)* the particular arrangement of calcite and aragonite lamellae oriented perpendicular inside the mussel shells[26]. From the compositional point of view, the major characteristic components (Ca, C and O) and also traces of Mg in the case of marble were identified. Materials may contain, additionally variable quantities of Na and/or Si given their environment, but here these were under the detection limit of the EDS device. The XRD patterns of raw materials are comparatively presented in **Fig. 3A**. They indicated the pure $CaCO_3$ phase by peaks with the maximum intensity at: 2θ = ~29.5°, 47-48° (marble – calcite, ICDD: 01-086-2339) and ~27°, 32.5°, 43° (seashells – aragonite, ICDD: 00-005-0453). For marble, characteristic $CaMg(CO_3)_2$ (ICDD: 00-036-0426) peaks were also identified at 37° and 42.5°; this confirms the presence of Mg on EDS analysis[27] . The comparative FT-IR spectra are shown in **Fig. 3B**. The IR absorption data also complement the XRD results. The characteristic vibrational bands of $CaCO_3$ were identified at: ν_2 and ν_3 asymmetric bending (~870 cm^{-1} and ~1460 cm^{-1} respectively), ν_4 symmetric bending (~700 cm^{-1}) and ν_1 symmetric stretching (~2360 cm^{-1} and 2900 cm^{-1}) modes of the CO_3^{2-} molecule. Further, the vibrational mode of environmentally-derived water molecules could be seen at ~3600 cm^{-1}. The results of thermal analysis TGA/DSC are presented in **Fig. 4**. Since the variable content of additional elements (e.g. Na, Si) could influence the dissociation temperature, thermal analysis was performed between 25 - 1400°C for a complete decomposition of both precursors. Correlative to morpho-compositional properties (**Fig.3**), results highlighted the characteristic thermal phenomena of phased decomposition (irreversible transformations): *1)* dolomite→calcite→calcium oxide (marble) and *2)* aragonite→calcite→calcium oxide (seashells). At around 75°C, on the DSC curve of marble sample, a characteristic peak for the environmentally-absorbed water

evaporation was identified. Dolomite decomposition to a more thermally stable phase (calcite) was an endothermic process (HF~ -1.25 W/g) which took place at T=307°C, with a weight loss of 1.91%. Similar decomposition of seashells (endothermic conversion of aragonite to calcite) happened at T=307°C (HF~ - 0.75 W/g), with a weight loss of 2.17%. Dissociation reactions proceeded up to 838°C and 899°C respectively. For seashells, the characteristic Gaussian (bell-shaped) peak indicated a fine crystalline structure; contrary, to marble sample. The characteristic split peak suggested the presence of larger crystals in the materials structure. These reactions were accompanied by a major thermal event: CO_2 loss reached a 42% of the sample mass. The remaining CaO mass was preserved up to a temperature of 1400°C. Hence, the established dissociation temperature was lower than the one of pure $CaCO_3$ minerals (963°C).

3.2 *Intermediary calcium oxide powder characterization*

Results of SEM-EDS analysis conducted before and after calcination process (**Fig. 1&5**) showed the changes induced by the heat treatment in the microstructure of marble and seashells. Marble`s morphology started with acute cracking of the initial microstructure (**Fig. 1**), while maintaining a high compactness degree (**Fig. 5, marble derived CaO**). In contrary, the seashells decomposition led to the particles interconnection in form of pores, through fragmentation and aeration of the component layers (**Fig. 5, seashell derived CaO**). Mechanical tension caused by induced hydration in atmospheric air for 6 months led to an architecture that was composed of independent grains in both cases[28]. The fine particles clogged in the form of crystals with variable, quasi-regular geometries and sizes in the range of 1-10 μm (**Fig. 5,** marble/seashell derived $Ca(OH)_2$). From the compositional standpoint, EDS analysis demonstrated the presence of the characteristic elements for such compound type (Ca, O), for both natural precursors. The XRD patterns of marble and seashell derived CaO powders are comparatively shown in **Fig. 5A**. In both cases, a single-phase structure composed of CaO (ICDD: 01-070-5490) was revealed. This suggests a complete dissociation of calcium carbonate at 1300°C. Atmospheric air exposure for 6 months led to partially hydration and therefore to a bi-phasic composition with the main phase consisting of $Ca(OH)_2$ (ICDD: 01-084-1271). FT-IR analysis confirmed this transformation CaO→Ca

$(OH)_2$ (**Fig. 5B**): characteristic CaO bands in the 1450-1700 cm^{-1} region presented modified shape and intensity[28].

3.3 Physico-chemical characterization of synthesized CaPs

Post synthesis, six powdery samples were obtained (**Fig. 6**). The liquid seashell-derived sample (2-S), resulted after doubling the amount of H_3PO_4 has been excluded from subsequent analyzes.

3.3.1 SEM/EDS analysis

The microstructure evolution of dried samples is presented in **Fig. 7**. A refined granulation can be easily observed for samples synthesized in the presence of magnetic stirring (see **Table 1**) by transition of conglomerate grains with sizes lower than 100µm (sample 0-M) to defined, needle-like ones with sizes around 50 µm (samples 1-M and 1-S). Moreover, in the absence of magnetic stirring crystallization, clusters were formed which led to incomplete conversion of $Ca(OH)_2$, as evidenced from XRD analysis in **Fig. 8**. At 1.5 x stoichiometric acid quantity, samples 1.5-M and 1.5-S displayed predominantly lamellar platelets and a small number of interposed needle-like particles with dimensions of less than 50 µm. For the seashell-derived samples, a proclivity to rounded platelets with a non-uniform size distribution could be observed. Further acid quantity increasing (sample 2-M) led to the conversion of lamellar platelets into grains with quasi-rounded complex shapes and varied dimensions (decreased by 75% compared to the previous ones). Agglomeration of small needle-like arrangements has defined a compact structure, with low porosity. The comparative EDS spectra (**Fig. 7**) highlighted the characteristic elements for CaPs (Ca, P and O). The Ca/P molar ratios values – calculated based on these results – varied between 0.91 - 1.53 and suggest an incomplete conversion of CaO powder into biogenic HA. As the acid quantity/sample increases, the Ca/P ratio and pH decrease and hence the final products consists also of acidic calcium phosphates. It should also be noted that the calculated Ca/P ratios can be influenced and slightly shifted by the instrument`s possible errors. They were maintained in the normal limits (below 0.1%) throughout analyzes[29] . In order to identify the obtained compounds, the calculated Ca/P ratios were correlated with XRD results.

3.3.2 Structural investigations

The XRD patterns of dried samples have been comparatively displayed in **Fig. 8A**. Among all stoichiometric synthesized samples, only the 1-M one (marble derived) showed a structure with 100% HA (ICDD: 01-089-6438). In the absence of magnetic stirring, sample 0-M evolved to a bi-phasic composition with HA (93%) coexisting with unreacted $Ca(OH)_2$ (ICDD: 01-070-6449). In the case of all the other samples prepared under non-stoichiometric conditions, results revealed a bi-phasic composition consisting of DCPA (ICDD: 01-071-1759) and a secondary HA phase. The pH drop (**Fig. 7**), from pH=7.2 (sample 1-M) to slightly acidic values (6.8 - 7) recorded after increasing the amount of H_3PO_4 favored the precipitation of DCPD and DCPA phases. The HA phase proportion progressively decreased in favor of DCPA as follows: 1.5-M – 34%, 2-M – 21%, 1-S – 25%, 1.5-S – 18% HA. The modification mechanism of phasic composition could occur *i)* indirectly – by initially forming the DCPD phase which after drying treatment is fully converted to DCPA or *ii)* directly – the precipitation of DCPA is supported by the initial solution`s high acidity[30]. For marble-derived samples, the DCPA formation may be linked to the inhibitory effect of Mg on HA growth which develops through the randomly interactions of $Ca_9(PO_4)_6$ clusters (Posners clusters") with the aqueous medium[31]. The DCPA proportion obtained by precursors conversion was in good agreement with its theoretical Ca/P ratio (1.0) [59, 60], except for the sample 1-M wherein the ratio (Ca/P= 1.53) corresponds to a non-stoichiometric HA. The absence of α-/β-TCP phases (generally present at 2θ=19-21°) is a good indicator for the chosen drying temperature (120°C). The FT-IR spectra have been comparatively presented in **Fig. 8B** for all synthesized samples. In all aspects, results are in agreement to those acquired by XRD. The HA characteristic bands were identified: ν_4 symmetric bending (~560 cm^{-1}), ν_1 symmetric stretching (~990 cm^{-1}) and ν_3 asymmetric stretching (~1050-1150 cm^{-1}) modes of orthophosphate functional groups, the vibrational mode of hydroxyl groups (~725 cm^{-1}, 3400-3550 cm^{-1})[32] and the corresponding HPO_4^{2-} bands positioned at ~900 cm^{-1} and 1400 cm^{-1}. The intensity amplification of the latter ones is directly correlated with the DCPA increasing proportion identified by XRD analysis. The DCPA presence in the materials structure is desirable due to its superior biological properties: DCPA scaffolds registered a higher resorption degree compared to apatite based cements and osteoconductive properties above DCPD based ones[30].

Bands positioned at about 2000-2300 cm^{-1} are characteristic for ν_3 bending mode of carbonate molecule and those from the 2900-3400 cm^{-1} region for the absorbed water.

4 CONCLUSIONS

The optimized Rathje method proposed in this study facilitated the calcium phosphates synthesis from dolomitic marble and *Mytilus galloprovincialis* mussel shell precursors. The calcination temperature together with pH and H_3PO_4 amount are the key parameters governing the performance of the adapted synthesis route for materials derived from natural resources. A complete dissociation was possible for both calcium carbonate-based precursors at 1300°C. The synthesis parameters favored a 100% HA phase proportion only in stoichiometric conditions with magnetic stirring and using marble derived powder with a refined microstructure. Increasing the H_3PO_4 amount led to the precipitation of bi-phasic HA/DCPA compounds in both cases. Overall, these results confirm the possibility of extending the natural precursors range for HA preparation and also bring forward an alternative synthesis for DCPA based cements. Used raw materials constitute a sustainable and cost-efficient source for the highly performing bio-ceramics fabrication, destined for medical applications. Additional investigations are required to thoroughly establish the optimum HA/DCPA ratio for a proper performance of the bi-phasic CaPs that will be reported in near future.

Acknowledgement: „ This work was supported by a grant of the Romanian National Authority for Scientific Research and Innovation, CNCS – UEFISCDI, project number PN-II-RU-TE-2014-4-0590", project acronym BIOMIMBONE.

References

[1] M. Ashaduzzaman, S.R. Deshpande, N.A. Murugan, Y.K. Mishra, A.P.F. Turner, A. Tiwari, On/off-switchable LSPR nano-immunoassay for troponin-T, Sci. Rep. 7 (2017). doi: 10.1038/srep44027.

[2] N. Duggal, D. Jaishankar, T. Yadavalli, S. Hadigal, Y.K. Mishra, R. Adelung, D. Shukla, Zinc oxide tetrapods inhibit herpes simplex virus infection of cultured corneas, Mol. Vis. 23 (2017) 26–38.

[3] V.K. Thakur, A.S. Singha, M.K. Thakur, Surface modification of natural polymers to impart low water absorbency, Int. J. Polym. Anal. Charact. 17 (2012) 133–143.

[4] A.S. Singha, V.K. Thakur, Synthesis and Characterization of Grewia Optiva Fiber-reinforced PF-based Composites, Int. J. Polym. Mater. Polym. Biomater. 57 (2008) 1059–1074. doi:10.1080/00914030802257800.

[5] V.K. Thakur, A.S. Singha, Natural fibres-based polymers: Part I—Mechanical analysis of Pine needles reinforced biocomposites, Bull. Mater. Sci. 33 (2010) 257–264. doi:10.1007/s12034-010-0040-x.

[6] V. K. Thakur, D. Vennerberg, S. A. Madbouly, M. R. Kessler, Bio-inspired green surface functionalization of PMMA for multifunctional capacitors, RSC Adv. 4 (2014) 6677–6684. doi:10.1039/C3RA46592F.

[7] W.C. Liu, S. Chen, L. Zheng, L. Qin, Angiogenesis Assays for the Evaluation of Angiogenic Properties of Orthopaedic Biomaterials - A General Review, Adv. Healthc. Mater. 6 (2017) UNSP 1600434. doi:10.1002/adhm.201600434.

[8] M.K. Thakur, V.K. Thakur, R.K. Gupta, A. Pappu, Synthesis and Applications of Biodegradable Soy Based Graft Copolymers: A Review, ACS Sustain. Chem. Eng. 4 (2016) 1–17. doi:10.1021/acssuschemeng.5b01327.

[9] A.S. Singha, V.K. Thakur, Fabrication and study of lignocellulosic hibiscus sabdariffa fiber reinforced polymer composites, BioResources. 3 (2008) 1173–1186.

[10] S.I. Voicu, R.M. Condruz, V. Mitran, A. Cimpean, F. Miculescu, C. Andronescu, M. Miculescu, V.K. Thakur, Sericin Covalent Immobilization onto Cellulose Acetate Membrane for Biomedical Applications, ACS Sustain. Chem. Eng. 4 (2016) 1765–1774.

[11] M.C. Corobea, O. Muhulet, F. Miculescu, I.V. Antoniac, Z. Vuluga, D. Florea, D.M. Vuluga, M. Butnaru, D. Ivanov, S.I. Voicu, others, Novel nanocomposite membranes from cellulose acetate and clay-silica nanowires, Polym. Adv. Technol. 27 (2016) 1586–1595.

[12] M. Miculescu, V.K. Thakur, F. Miculescu, S.I. Voicu, Graphene-based polymer nanocomposite membranes: a review, Polym. Adv. Technol. 27 (2016) 844–859. doi:10.1002/pat.3751.

[13] J. Venkatesan, S.-K. Kim, Nano-Hydroxyapatite Composite Biomaterials for Bone Tissue Engineering-A Review, J. Biomed. Nanotechnol. 10 (2014) 3124–3140. doi:10.1166/jbn.2014.1893.

[14] D.M. Roy, S.K. Linnehan, Hydroxyapatite formed from Coral Skeletal Carbonate by Hydrothermal Exchange, Nature. 247 (1974) 220–222. doi:10.1038/247220a0.

[15] S. Santhosh, S.B. Prabu, Synthesis and characterisation of nanocrystalline hydroxyapatite from sea shells, Int. J. Biomed. Nanosci. Nanotechnol. 2 (2012) 276–283. doi:10.1504/IJBNN.2012.051221.

[16] L. Ferrage, G. Bertrand, P. Lenormand, D. Grossin, B. Ben-Nissan, A review of the additive manufacturing (3DP) of bioceramics: alumina, zirconia (PSZ) and hydroxyapatite, J. Aust. Ceram. Soc. 53 (2017) 11–20. doi:10.1007/s41779-016-0003-9.

[17] A. Haider, S. Haider, S.S. Han, I.-K. Kang, Recent advances in the synthesis, functionalization and biomedical applications of hydroxyapatite: a review, Rsc Adv. 7 (2017) 7442–7458. doi:10.1039/c6ra26124h.

[18] F. Abbona, H.E. Lundager Madsen, R. Boistelle, The final phases of calcium and magnesium phosphates precipitated from solutions of high to medium concentration, J. Cryst. Growth. 89 (1988) 592–602. doi:10.1016/0022-0248(88)90223-0.

[19] M.-P. Ginebra, C. Canal, M. Espanol, D. Pastorino, E.B. Montufar, Calcium phosphate cements as drug delivery materials, Adv. Drug Deliv. Rev. 64 (2012) 1090–1110. doi:10.1016/j.addr.2012.01.008.

[20] W.-C. Chen, J.-H.C. Lin, C.-P. Ju, Transmission electron microscopic study on setting mechanism of tetracalcium phosphate/dicalcium phosphate anhydrous-based calcium phosphate cement, J. Biomed. Mater. Res. A. 64 (2003) 664–671. doi:10.1002/jbm.a.10250.

[21] Y.P. Guo, Y. Zhou, Conversion of nacre powders to apatite in phosphate buffer solutions at low temperatures, Mater. Chem. Phys. 106 (2007) 88–94. doi:10.1016/j.matchemphys.2007.05.022.

[22] H. Onoda, S. Yamazaki, Homogenous hydrothermal synthesis of calcium phosphate with calcium carbonate and corbicula shells, J. Asian Ceram. Soc. 4 (2016) 403–406. doi:10.1016/j.jascer.2016.10.001.

[23] F. Tamimi, Z. Sheikh, J. Barralet, Dicalcium phosphate cements: brushite and monetite, Acta Biomater. 8 (2012) 474–487. doi:10.1016/j.actbio.2011.08.005.

[24] S.V. Dorozhkin, Biphasic, triphasic and multiphasic calcium orthophosphates, Acta Biomater. 8 (2012) 963–977. doi:10.1016/j.actbio.2011.09.003.

[25] S. Pina, S.I. Vieira, P. Rego, P.M.C. Torres, O. a. B. da Cruz e Silva, E.F. da Cruz e Silva, J.M.F. Ferreira, Biological responses of brushite-forming Zn- and ZnSr-substituted beta-tricalcium phosphate bone cements, Eur. Cell. Mater. 20 (2010) 162–177.

[26] G.M. Luz, J.F. Mano, Mineralized structures in nature: Examples and inspirations for the design of new composite materials and biomaterials, Compos. Sci. Technol. 70 (2010) 1777–1788. doi:10.1016/j.compscitech.2010.05.013.

[27] M. Samtani, D. Dollimore, K. Alexander, Thermal Decomposition of Dolomite in an Atmosphere of Carbon Dioxide: The effect of procedural variables in thermal analysis, J. Therm. Anal. Calorim. 65 (2001) 93–101. doi:10.1023/A:1011572401137.

[28] M. Galvan-Ruiz, J. Hernandez, L. Banos, J. Noriega-Montes, M.E. Rodriguez-Garcia, Characterization of Calcium Carbonate, Calcium Oxide, and Calcium Hydroxide as Starting Point to the Improvement of Lime for Their Use in Construction, J. Mater. Civ. Eng. 21 (2009) 694–698. doi:10.1061/(ASCE)0899-1561(2009)21:11(694).

[29] P.J. Statham, The generation, absorption and anisotropy of thick-target bremsstrahlung and implications for quantitative energy dispersive analysis, X-Ray Spectrom. 5 (1976) 154–168. doi:10.1002/xrs.1300050310.

[30] M. Montazerolghaem, M. Karlsson Ott, H. Engqvist, H. Melhus, A.J. Rasmusson, Resorption of monetite calcium phosphate cement by mouse bone marrow derived osteoclasts, Mater. Sci. Eng. C Mater. Biol. Appl. 52 (2015) 212–218. doi:10.1016/j.msec.2015.03.038.

[31] S. Jalota, S.B. Bhaduri, A.C. Tas, Osteoblast proliferation on neat and apatite-like calcium phosphate-coated titanium foam scaffolds, Mater. Sci. Eng. C. 27 (2007) 432–440. doi:10.1016/j.msec.2006.05.052.

[32] M. Markovic, B.O. Fowler, M.S. Tung, Preparation and Comprehensive Characterization of a Calcium Hydroxyapatite Reference Material, J. Res. Natl. Inst. Stand. Technol. 109 (2004) 553–568. doi:10.6028/jres.109.042.

Highlights

- Physico-chemical processing of calcium-rich resources can be achieved by Rathje method adaptation
- Dolomitic marble and mussel seashells stand as a new eco-sustainable alternative for biological calcium phosphate-based cements manufacturing
- Magnetic stirring presence along with the reagent amount and pH control proved imperative for the final synthesized HA phase proportion

Table 1: *HA synthesis parameters according to adapted Rathje method*

Sample		0-M	1-M	1.5-M	2-M	1-S	1.5-S	2-S
Parameter	$Ca(OH)_2$ [g]	2	2	2	2	2	2	2
	H_3PO_4 [ml]	1.33	1.33	2	2.66	1.33	2	2.66
	Magnetic stirring [2h]	x	✓	✓	✓	✓	✓	✓

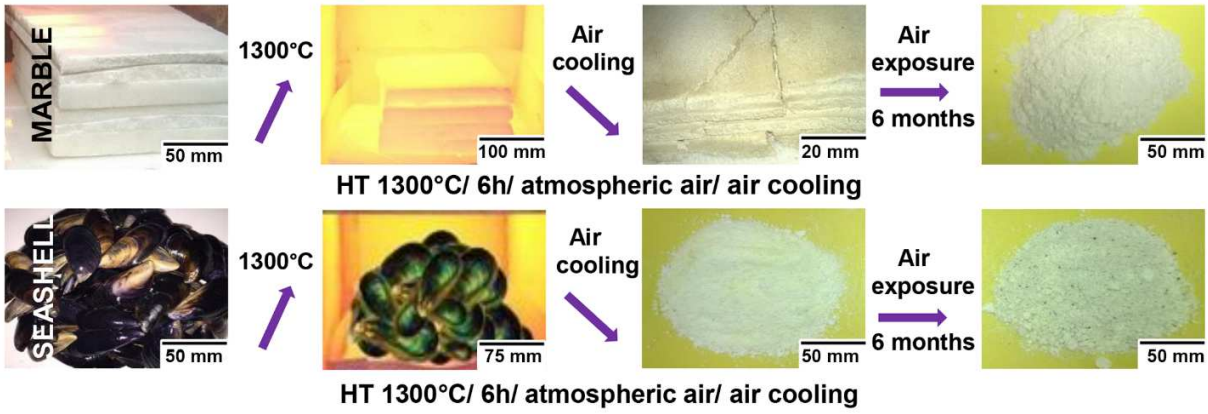

Fig.1: Parameters for conversion process of natural $CaCO_3$ based – materials to CaO, prior to Rathje method implementation

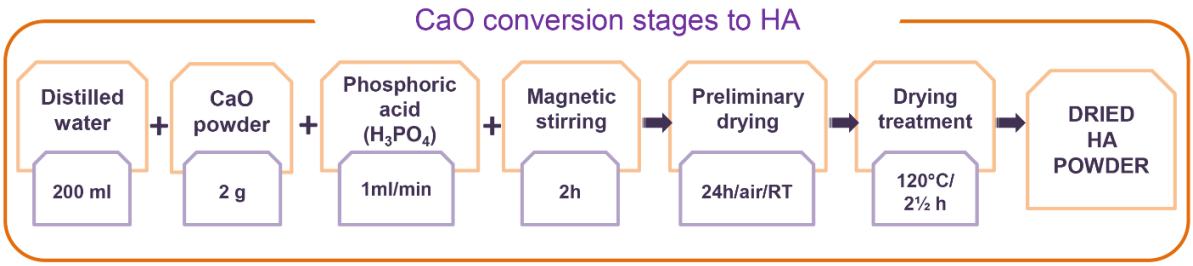

Fig.2: Stages and working parameters for CaO conversion to biogenic HA through modified Rathje method

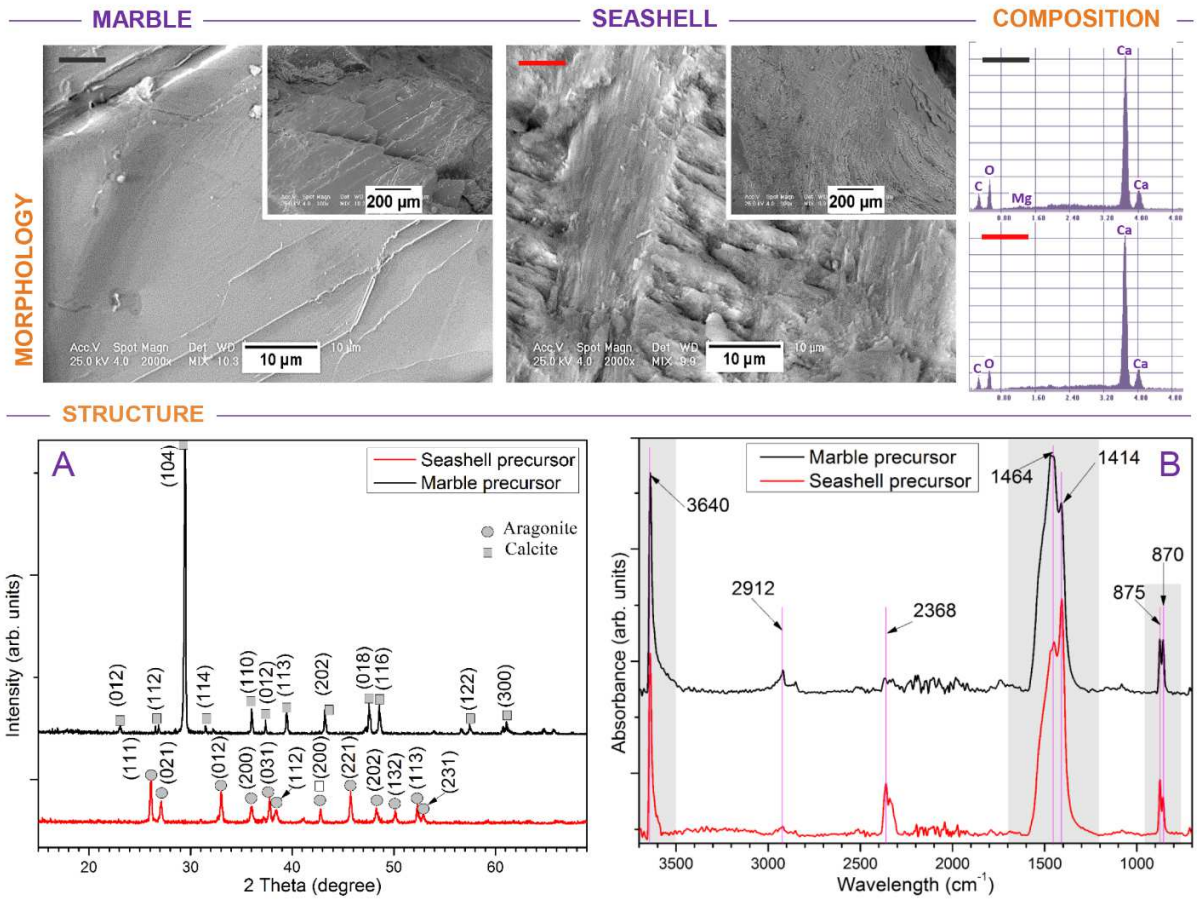

Fig.3: Marble and seashells` characterization: morphological SEM/EDS and structural by FT-IR (A), XRD (B), performed prior to thermal dissociation at 1300°C

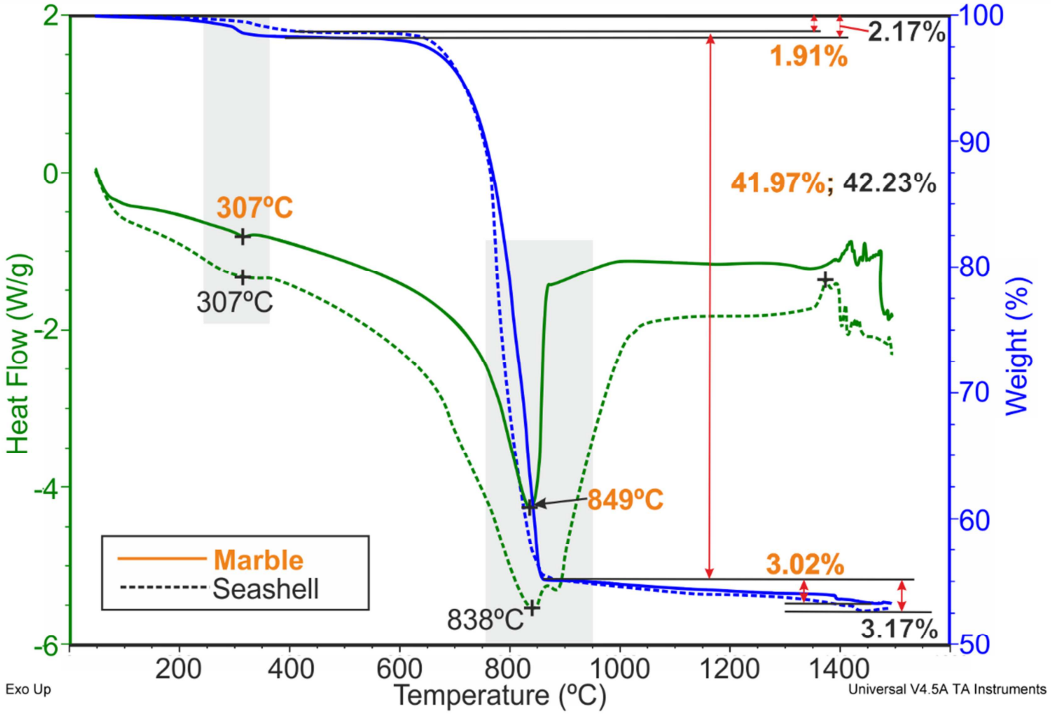

Fig.4: TGA-DSC analysis performed on targeted natural precursors: marble and seashells

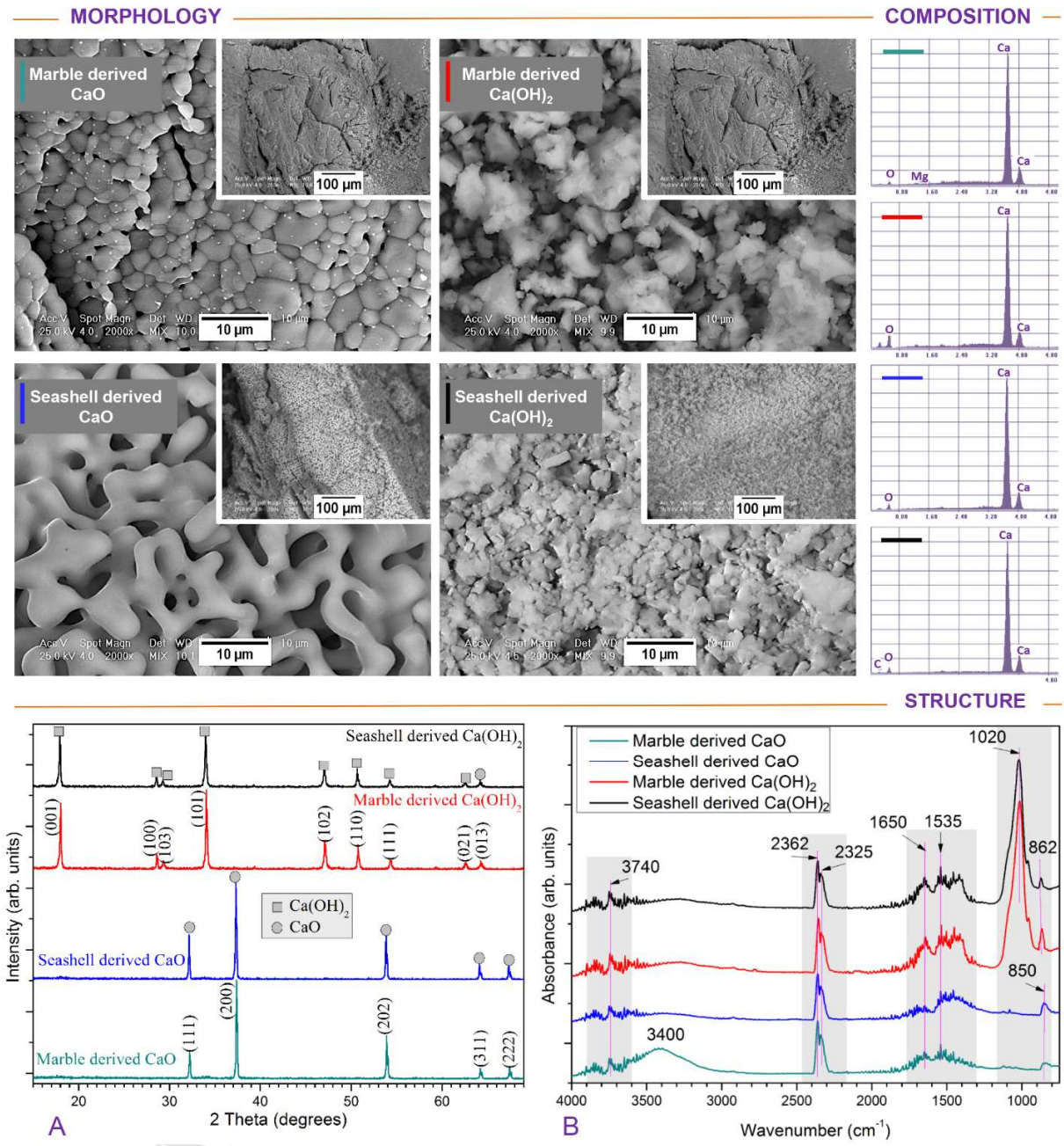

Fig.5: CaO powder characterization: morphological SEM/EDS and structural XRD (A), FT-IR (B), performed after $CaCO_3$ thermal dissociation at 1300°C

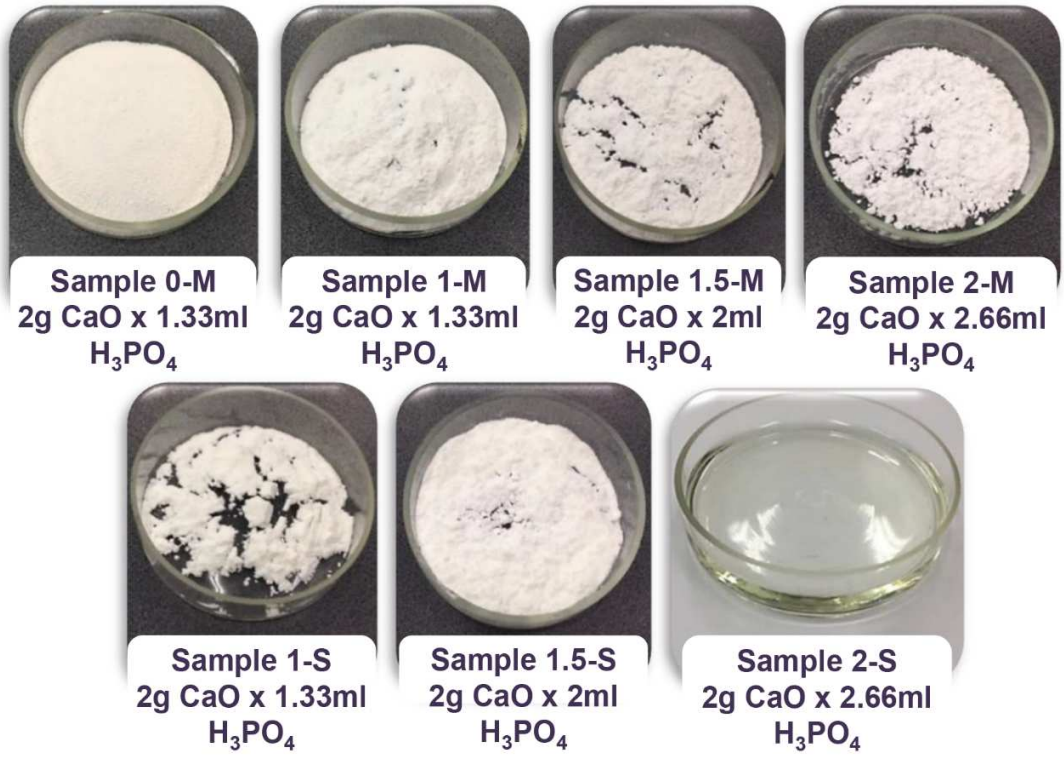

Fig.6: Visual aspect of synthesized HA samples through modified Rathje method; photographs were taken after the final drying treatment

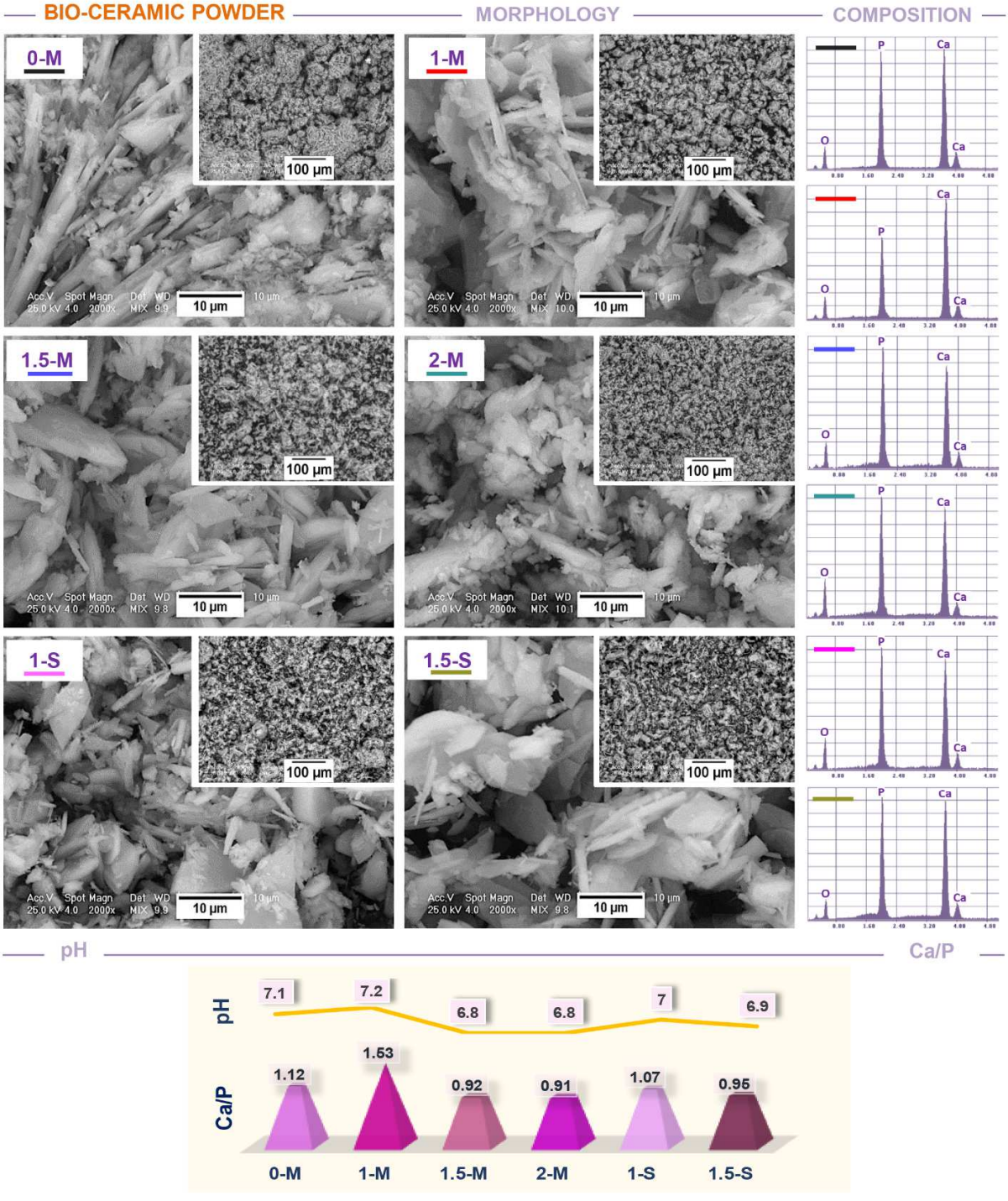

Fig.7: Morpho-compositional analysis of ceramic powdery samples obtained through modified Rathje method; investigations were conducted after the final drying treatment

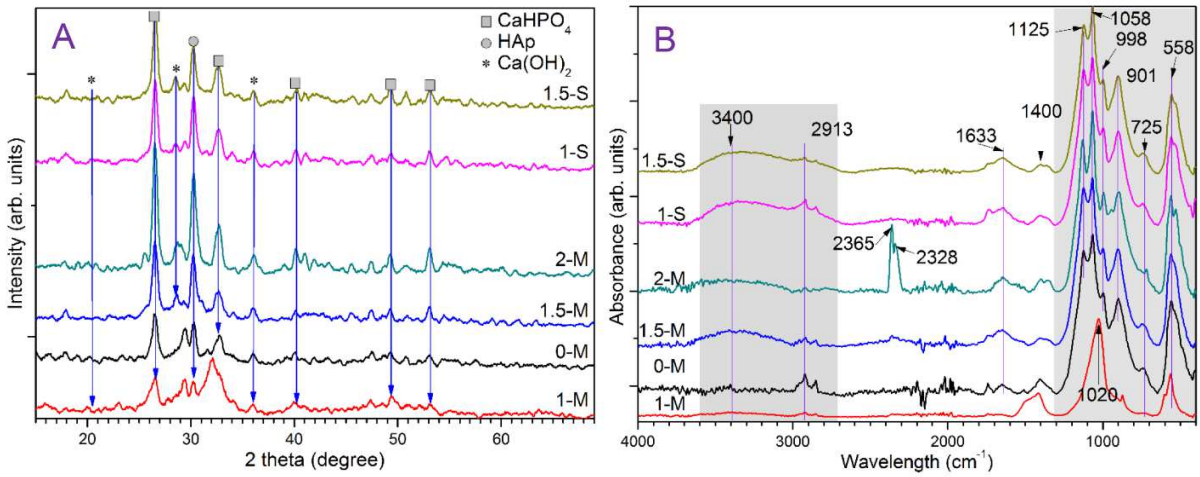

Fig.8: Structural investigations of bio-ceramic samples: XRD (A), FT-IR (B), obtained through modified Rathje method; investigations were conducted after the final drying treatment

2017-06-07

Facile synthesis and characterization of hydroxyapatite particles for high value nanocomposites and biomaterials

Miculescu, Florin

Elsevier